Adsorption of Polyethylenimine on Graphite: An Atomic Force Microscopy Study

Marc Schneider,* Martin Brinkmann, and Helmuth Möhwald

Max-Planck-Institut für Kolloid- und Grenzflächenforschung, Am Mühlenberg, D-14476 Golm, Germany

Received April 24, 2003; Revised Manuscript Received September 18, 2003

ABSTRACT: The adsorption of the weak and branched polyelectrolyte polyethylenimine (PEI) on planar, uncharged graphite surfaces is investigated with the atomic force microscope (AFM). The high lateral resolution of the AFM allows for the observation of single molecules adsorbed to the surface from diluted solutions. Different adsorption structures were found in dependence of the pH value of the solution and the incubation time of the adsorption process. Patterns of individual PEI molecules are due to repulsive interactions. These interactions result in a main intermolecular distance and highly ordered stringlike structures. Equal intermolecular distances for all pH values reveal the ability of the PEI molecules to adjust their charge density. Dipolar interactions explain the high ordering of the molecules. Furthermore, the superimposing influence of the hexagonal graphite lattice can be observed for long adsorption times.

Introduction

For decades, polymers and especially polyelectrolytes have received a lot of attention because of their vast number of possible applications. They were widely used in paper industries,[1,2] in the food industry,[3,4] in life sciences,[5] and for gene transfer in molecular medicine.[6−8] For many of the uses, the adsorption of polyelectrolytes to a surface and the alteration of the surface properties are important issues. Additionally, the adsorption properties of polyelectrolytes on different substrates and the dependence of the adsorption on the environment are of high scientific interest. It is therefore necessary to understand the process of adsorption on the scale of single molecules.

First approaches for the adsorption of weak polyelectrolytes were introduced by Evers et al.[3] and extended by Böhmer et al.[9] For surfaces of opposite charge to the polyelectrolytes, flat adsorption configurations, e.g., in refs 10−12, and a slight overcharging, e.g., in refs 9 and13, are observed experimentally and theoretically. In the absence of electrostatic interactions between the molecules and the surface, the parameter χ_S, introduced by Silverberg[14] and Roe,[15] determines if and to what extent adsorption will occur. However, not much direct experimental data on the adsorption process of weak polyelectrolytes are available.[16]

Most often the adsorption is followed by averaging methods such as optical reflection or scattering techniques[17−19] and quartz crystal microbalance (QCM) studies.[20−22] In contrast, scanning probe techniques offer the unique possibility to look at the adsorption on the nanometer scale. There is, in principle, no limitation in the resolution of AFM due to small adsorbed amounts that would exclude investigation of the adsorption at the beginning of the adsorption process or of the adsorption from very dilute solutions. The quantification of for example sizes of single molecules allows for following the adsorption process in detail. These data make it possible to draw conclusions on the relevant interactions of the molecules.

The polyelectrolyte we have chosen for investigation, polyethylenimine (PEI), is a technically important, branched, polydisperse polyelectrolyte. Despite its importance, its behavior is still not fully understood theoretically.[23−25]

* Corresponding author: e-mail Marc.Schneider@mpikg-golm-.mpg.de.

Methods

Chemicals. Branched polyethylenimine with a molecular weight of M_w = 750 000, purchased from Sigma-Aldrich (Deisenhofen, Germany), was used as obtained. The polymer features three different types of amino groups: primary, secondary, and tertiary amino groups. The ratio of primary-to-secondary-to-tertiary amino groups is 1:2:1.[26,27] In addition, the polyethylenimine molecules show a polydisperse character ($M_w/M_n \sim 12$). An additional very important feature is the compactness of the molecules because of their globular architecture. This can be seen as well from the Mark−Houwink relation ($R_G \sim M_w^{0.44}$) and the very small exponent.[28] In the case of a hard sphere $R_G \sim M_w^{0.33}$ and for a stiff rod $R_G \sim M_w^{1}$.

Atomic Force Microscopy (AFM). A scanning force microscope (Nanoscope Multimode IIIa, Digital Instruments, Santa Barbara, CA), silicon cantilevers (Nanosensors, Wetzlar, Germany), and silicon cantilevers coated with aluminum on the back (Olympus Optical Co. Ltd., Tokyo, Japan) with typical resonance frequencies around 300 kHz and spring constants around 40 N/m were applied.

Structure and particle size analysis were done with the DI software. Statistical calculations were performed with a stochastic freeware program from Prof. Stoyan (Freiberg University, Germany).

Sample Preparation. Graphite supports (HOPG ZYH grade, Advanced Ceramics, Lakewood, OH) were used as substrates. 10−30 μL of an aqueous polymer solution ([c] $\sim 4 \times 10^{-5}$ g/L) was deposited on the substrate. The polymer was allowed to adsorb on the surface for different times: from several seconds to 24 h. To avoid changes of the concentration for long adsorption times, the substrate with the drop of polyelectrolyte solution was placed in a saturated atmosphere. Because of the absence of strong binding to the surface due to electrostatic interactions, the drying process has to be gentle. Drying by blotting with tissue paper provides an appropriate method to adhere molecules on a graphite surface.[29]

All measurements were performed at ambient conditions in air. For investigations under liquid the adsorption forces of the molecules on the graphite surface were too small; the molecules were moved by the cantilever on the surface.

Results and Discussion

The adsorption behavior of PEI molecules on hydrophobic and uncharged graphite was investigated for different incubation times, from seconds up to 24 h. For

10.1021/ma0345293 CCC: $25.00
Published on Web 10/23/2003

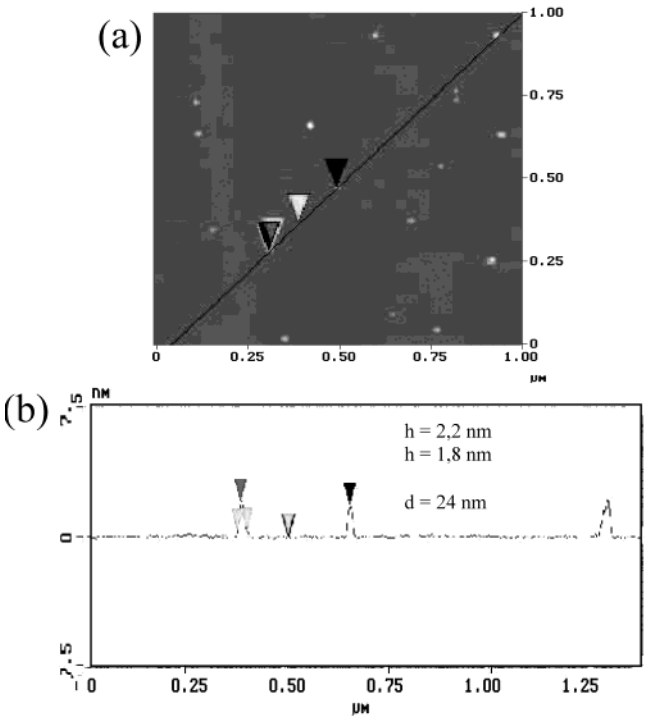

Figure 1. (a) Micrograph of single PEI molecules adsorbed on graphite. The polyelectrolyte solution of pH = 3 was allowed to incubate the surface for $t = 30$ s. (b) Cross section along the line in (a). The molecules have a height of $h = 2$ nm and a lateral size of $d = 24$ nm.

short adsorption times the molecules show an adsorption structure of well-separated single molecules (Figure 1a). The fact that we deal with single molecules can be deduced from the size of the molecules measured with the scanning force microscope (SFM) (Figure 1b). The radius of the adsorbed structures lies in the range of radii calculated from light scattering data.[27,30−33] An estimation of the mass of the adsorbed structures gives an additional hint that single molecules were adsorbed. From the measured volume $V_{meas} = 982$ nm^3 (the molecules are considered as cylinders) and the assumed density of the molecules, the mass can be estimated. The density of the PEI molecules in solution, provided by the producer, is 1.07 g/mL. The density of the adsorbed molecules should increase in comparison to the solution value because of the collapse of the molecules induced by the drying process ($\rho_c = 1.2$ g/mL). With these values, the mass of the adsorbed structures is approximately 650 kDa. If we take the polydispersity and the uncertainty of the density of the adsorbed molecules into account, the estimated molar mass is reasonable. These results confirm the fact that single molecules were adsorbed on graphite.

Comparing the dimensions of the adsorbed PEI molecules on graphite with those of the molecules adsorbed on a charged mica surface, we found a remarkable difference. On both substrates we discovered the expected and well-known flat (pancakelike) adsorption structures.[10−12,34−36] But on mica the effect is more pronounced than on graphite. Figure 2 depicts a height image of single molecules of PEI adsorbed on a mica surface. The average lateral size of the molecules is $\bar{r} = 20$ nm, and the average height is $\bar{h} = 0.6$ nm. The average radii of the molecules are larger on mica than graphite, whereas the height shows the opposite behavior. The height of the adsorbed molecules on graphite is higher than on mica. Because of the effect of convolution effects from the tip, care should be taken when lateral sizes are compared. To avoid mistakes due to the tip size, it is often more reliable to look at the height data of the adsorbed polyelectrolytes. However, on graphite we found an enormous variation in the heights of the adsorbed PEI molecules for different samples, each sample prepared with a fixed pH value, concentration, and the same incubation time. For this reason, the heights of the adsorbed molecules are not appropriate for a quantitative comparison. However, the lateral sizes of the imaged particles are altered in dependence of the tip size and the height of the object. Formula 1 describes the increase of the radius corresponding to the tip radius R_{tip} and the height of the imaged object h. The tip is thereby approximated with a sphere.

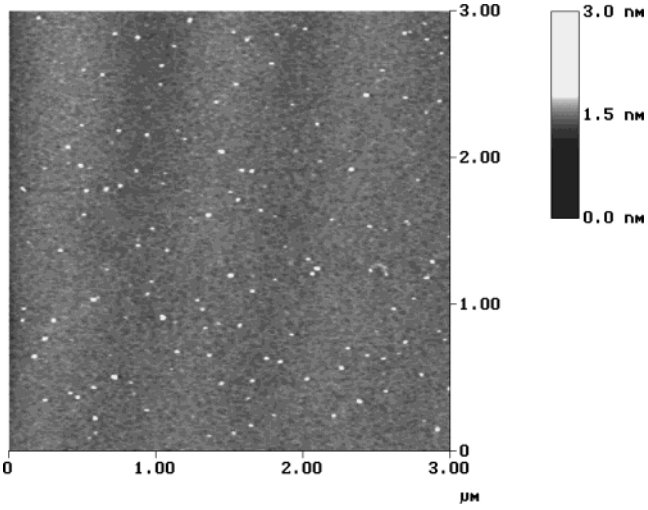

Figure 2. Topography image of single PEI molecules adsorbed on mica. The molecules were adsorbed from a solution of pH ~ 6. (Details for the sample preparation are given in refs 36 and 52.) The molecules show average lateral sizes of $r = 20$ nm and average heights of $h = 0.6$ nm.

$$\Delta R = \sqrt{{R_{tip}}^2 - (R_{tip} - h)^2} \qquad (1)$$

For a tip radius $R_{tip} = 15$ nm and an object height of 2 nm, one obtains an increase of $\Delta R = 7.5$ nm. For the same tip and an object with $h = 0.6$ nm one finds only $\Delta R = 4.2$ nm. Although the differences in the lateral sizes of the PEI molecules are within the error caused by convolution effects, the tendency of the measurements show a clear direction. The increase of the lateral size of the molecules is more pronounced on graphite due to the larger height. The molecules are, however, clearly smaller than on mica. This justifies the conclusion that the adsorbed molecules on graphite have smaller radii and larger heights than on mica.

This small but distinct difference can be ascribed to electrostatic interactions between the molecules and the mica surface in one case and to the absence of those in the case of the graphite surface. Figure 3 illustrates the adsorption of a branched and charged PEI molecule (globular architecture) in the presence and absence of surface charges, respectively. In solution the molecules are swollen, inter alia, because of segment−segment repulsion between the charged groups of each molecule. In the case of adsorption to the surface, the molecule collapses. On the oppositely charged mica surface, the PEI molecules compensate their charges with surface charges. Hence, they spread on the surface as much as

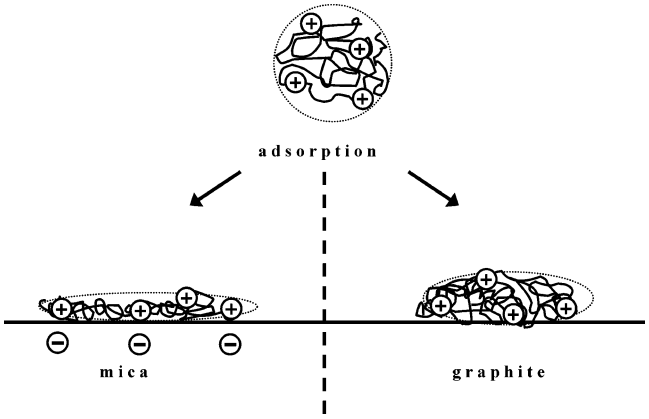

Figure 3. Sketch of a branched globular PEI molecule adsorbed from solution to graphite and mica. The molecule features a positive charge in solution. In the case of adsorption to the surface, the molecule collapses. On the oppositely charged mica surface, the PEI molecule compensates its charges by spreading on the surface as much as possible. A pronounced pancakelike structure is the consequence. On the graphite support the charged molecule segments are not compensated by the surface. Thus, the repulsive interaction is increased compared to mica.

possible. A pronounced pancakelike structure is the consequence.

On the graphite support the charged molecule segments cannot be compensated for by the surface. Therefore, the repulsive interaction within the molecules is increased compared to mica. The segment−segment repulsion leads in this case, to arrange the charges in an optimal way, to a bulkier adsorption structure. Unfortunately, a test of this hypothesis on an uncharged mica surface (at pH = 2) is not possible. The weak polyelectrolyte character of PEI entails an increasing charge density in the molecule with decreasing pH value. From pH = 3 the charge of the molecule is big enough to attract counterions.[31] This results in smaller sizes of the molecules in solution. One would therefore expect smaller adsorption structures as well, which would mask the effect.

A further interesting feature is the adsorbed amount of polyelectrolyte. On the uncharged graphite surface the amount of polymer adsorbed, in dependence of the charge density of the molecules, is easily accessible. On the contrary, on charged surfaces, where in addition the overall charge density changes with the pH value, the investigation of the adsorbed amount depends on several parameters.

Figure 4 shows a series of three AFM topography images taken after adsorption from three different pH values: a low value at pH = 3, an intermediate at pH ∼ 6, and a high value at pH = 11. One can see that the number of molecules adsorbed on the surface is increasing with decreasing degree of protonation. This effect is even more pronounced due to the decrease in incubation time.

The adsorption process of PEI molecules to the surface can be divided into three different steps: diffusion toward the surface, sticking to the surface, and rearrangement at the surface. The latter part is usually on much longer time scales[16,37] and is not relevant here.

The diffusion process has an important impact on the adsorption process. The diffusion constants of polyelectrolytes in dilute solutions change with the charge density of the molecule. A higher ion concentration increases the diffusion coefficient in solution.[38] The

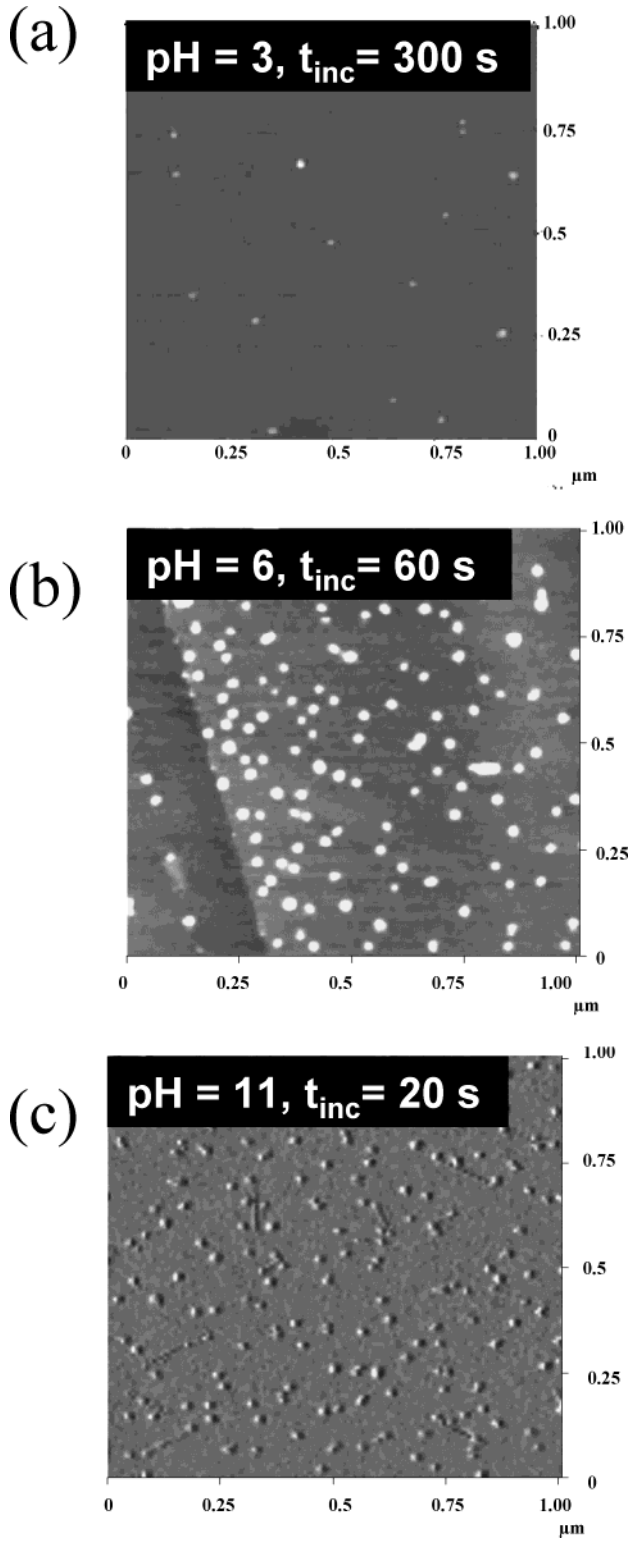

Figure 4. Three topography micrographs of PEI molecules adsorbed on graphite. (a) depicts the molecule distribution after adsorption from a solution of pH = 2 for t = 300 s. (b) shows PEI molecules adsorbed from pH ∼ 6 and t = 30 s. (c) shows the molecule distribution for adsorption from pH = 11 for t = 20 s. The adsorbed amount increases with increasing pH value though adsorption time is reduced.

hydrodynamic effects due to the change of the molecular size are more complicated for linear polymers; they change their shape and that influences the diffusion. In the case of the PEI molecules this can be neglected. The branched architecture mainly allows a radial swelling of the molecule. For this reason the diffusion of

single PEI molecules can be described with the well-known eq 2 for the diffusion coefficient.

$$D = \frac{k_B T}{6\pi\eta r_H} \tag{2}$$

The diffusion coefficient D is proportional to the thermal energy $k_B T$ and inversely proportional to the viscosity of the solvent, η, and the hydrodynamic radius of the diffusing object, r_H. Following data given by Horn,[31] the increase of the size of PEI molecules due to pH changes is around 50%. As a consequence, the diffusion coefficient is decreased by a factor of 1.5. Even a swelling to double the original radius would not significantly influence the diffusion. The time scales of the present adsorption experiments differ by more than a factor of 2. Hence, the different diffusion velocities are negligible. If the adsorption is diffusion limited, it can be shown that the adsorbed amount is proportional to the square root of the adsorption time and the diffusion coefficient.[39,40] This is not the case for the PEI adhering to graphite. Thus, diffusion of the molecules does not significantly affect the process.

Accordingly, the time dependence of the adsorption can be accounted for by different sticking probabilities. These sticking probabilities should be correlated with the segment−segment interaction of the adsorbing polyelectrolyte.

The adsorption behavior of the molecules we observed is in good agreement with the theoretical prediction for the adsorption of all kind of polyelectrolytes on uncharged surfaces.[41,42] This also holds for weak polyelectrolytes. The adsorbed amount is low for high intramolecular segment−segment repulsion. PEI at low pH values is highly charged and shows a strong repulsive interaction between the charged segments. The adsorbing and in consequence collapsing molecule has to overcome the energy barrier due to repulsion. An adsorption event is therefore much more unlikely. With decreasing charge density the repulsive force is reduced and the adsorbed amount per time is increased until a maximum is reached for uncharged molecules.

For a reasonable comparison of the adsorbed amount of polyelectrolyte in dependence of the pH value, it is necessary to normalize the data by the incubation time. Too long incubation times have to be excluded because of the influence of the adsorption-inhibiting electrostatic barrier,[42] which is present around each molecule. In Figure 5a the surface density ρ per second in percent of the total area is depicted in relation to the pH value. The adsorbed amount per time increases slightly for high charge densities of the PEI molecules and levels off for fully uncharged molecules (around pH = 10). The shape of the adsorption curve is the same as found for theoretical predictions for the adsorption of weak polyelectrolytes on uncharged surfaces.[3,9,43−45]

The curve in Figure 5a reflects the above-described influence of the segment−segment repulsion on the adsorption and indicates a positive adsorption parameter χ_S[14,15] at all pH values to graphite. We can fit our data (Figure 5b) following Fleer[45] and using the formula used for weak polyelectrolytes

$$\theta_{sp} = 1 - \frac{3}{2}\frac{e^{y-\chi_S}}{z + (1-z)e^{y}} \tag{3}$$

to calculate the adsorbed amount θ_{sp}. Here z is the segment charge of the molecule and y the surface potential of the modified surface by adsorption, which is different for each pH value and depends on the salt concentration, i.e., ionic strength. Fleer as well as Cohen Stuart et al.[42] used an implicit equation to express y as a function of the salt concentration and the segment charge

$$z\theta_{sp} = z\left(1 - \frac{3}{2}\frac{e^{y-\chi_S}}{z + (1-z)e^{y}}\right) = \frac{2}{3}0.67\sqrt{c_S}\,\sinh\left(\frac{y}{2}\right) \tag{4}$$

Fitting of the data provides a value for the nonelectrostatic adsorption parameter, $\chi_S \sim 1.3$. The ionic strength was adjusted according to the different pH values. This resulted in several intervals for the ionic strength in dependence of the pH and the segment charge: $[z_i,z_j] \rightarrow [\Phi_s]$: $[0-0.1] \rightarrow 10^{-3}$, $[0.1-0.2] \rightarrow 10^{-4}$, $[0.2-0.6] \rightarrow 10^{-6}$, $[0.6-0.7] \rightarrow 10^{-4}$, and $[0.7-1] \rightarrow 10^{-3}$. An additional assumption was made for χ_S, which is taken to be independent of the ionic strength. For the fitting procedure, the surface density ρ at pH = 11 was regarded (in the theoretical model) as the corresponding value for a fully covered surface ($\theta_{sp} = 1$). All adsorption

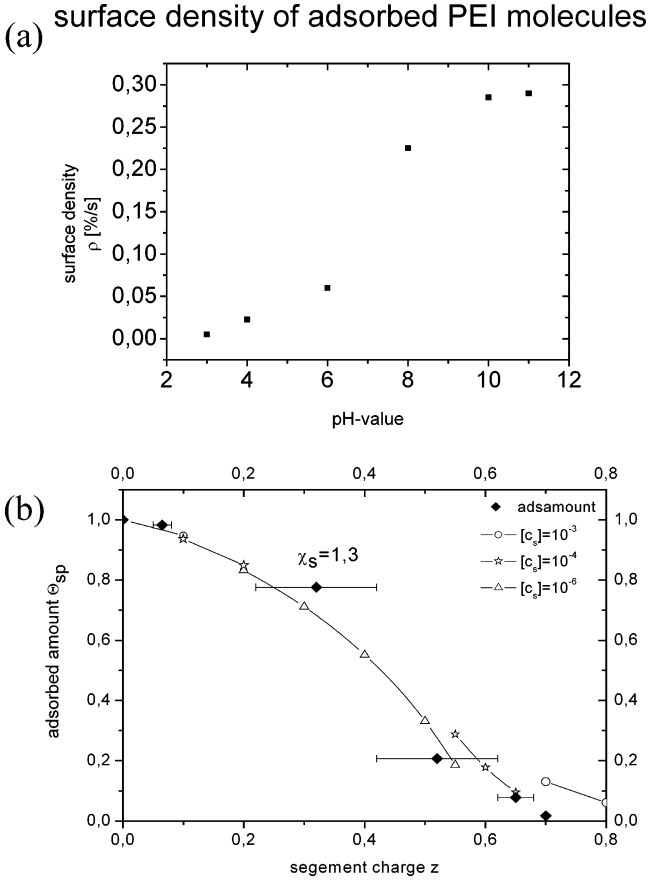

Figure 5. (a) Surface density per time of PEI molecules over the pH value of the stock solution. The dots represent the percentage of the surface that is covered with PEI as measured with the SFM. A bearing analysis was performed to determine the surface coverage. (b) Comparison between the experimental data (adsorbed amount in dependence of the segment charge of the PEI molecules) and the theoretical model for the description of the adsorption at uncharged surfaces. The (◆) dots represent the experimental data for the adsorbed amount. The straight lines with symbols stand for the fits to the data ($\chi_S \sim 1.3$) The different symbols of the fit curves result from different ionic strength (in dependence on the pH value: (○) → 10^{-3}, (☆) → 10^{-4}, and (△) → 10^{-6}). The error bars for the segment charge result from different literature values.[24,37,53]

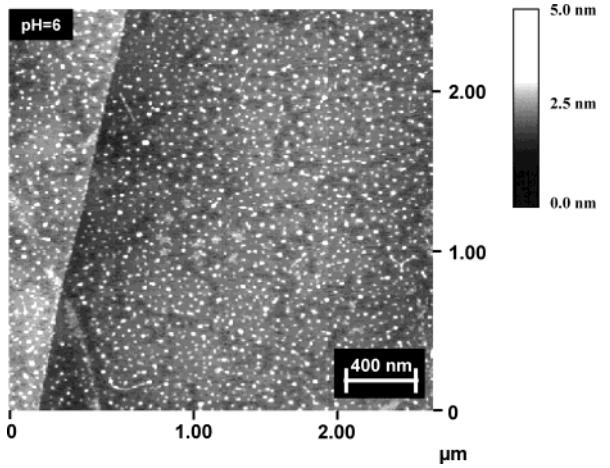

Figure 6. Typical micrograph displaying the topography of PEI molecules adsorbed on a graphite surface for pH < 8 after long incubation times. In this case, the adsorption is done from pH ~ 6 for t_{inc} > 20 min. The image depicts mainly well-separated single molecules.

data were normalized by this specific maximum value. The biggest difference to the experimental data is obtained for segment charges above $z = 0.6$. This is probably due to PEI's maximum degree of protonation of around 70%. Furthermore, the condensation of counterions modifies the electrostatic interaction between the segments, which then corresponds to a smaller ionic strength than indicated by the pH value.

For higher adsorbed amounts, single, separated molecules are still found. The distribution of the molecules can be investigated by means of statistical correlation functions. The pair-correlation function of the center coordinate of each molecule on the surface allows to determine whether a distance correlation exists between the molecules. Additional information can be obtained from the distance distribution of the nearest neighbor. In Figure 6 an adsorption pattern of PEI molecules is depicted. The molecules are adsorbed from a solution of pH ~ 6 for t_{inc} > 20 min. The pair-correlation and the distance distribution of the next neighbor obtained for this image are shown in Figure 7. It can be seen that the molecules show a preferred intermolecular distance due to the interaction among each other. The peak of the pair-correlation function $g(r)$ is located at a distance $d_{pc} = 103 \pm 10$ nm, with the error from the uncertainty in the peak position. The difference between the value obtained from the pair-correlation and the value from the distribution of the next neighbor is due to the different evaluation processes employed. The pair-correlation function takes all next neighbors into account whereas the distribution of the next neighbor only considers the nearest neighbor. The stronger and more reliable value for the intermolecular distance is therefore the pair-correlation value.[46] Nevertheless, the distribution of the next neighbor, d_{pc} > molecular diameter, confirms the fact that repulsive interactions are present. These forces are reflected in the shift of the peak to higher distances between the molecules when compared to a completely randomly arranged molecule pattern, as represented by the dashed line.[46,47] Comparing the maxima of the distances of the next-neighbor distribution of all pH values, we found repulsive interactions for all adsorption patterns from solution. In the case of the unprotonated PEI molecules, dipolar interactions or image charge effects can be made responsible for the internal order of the adsorption

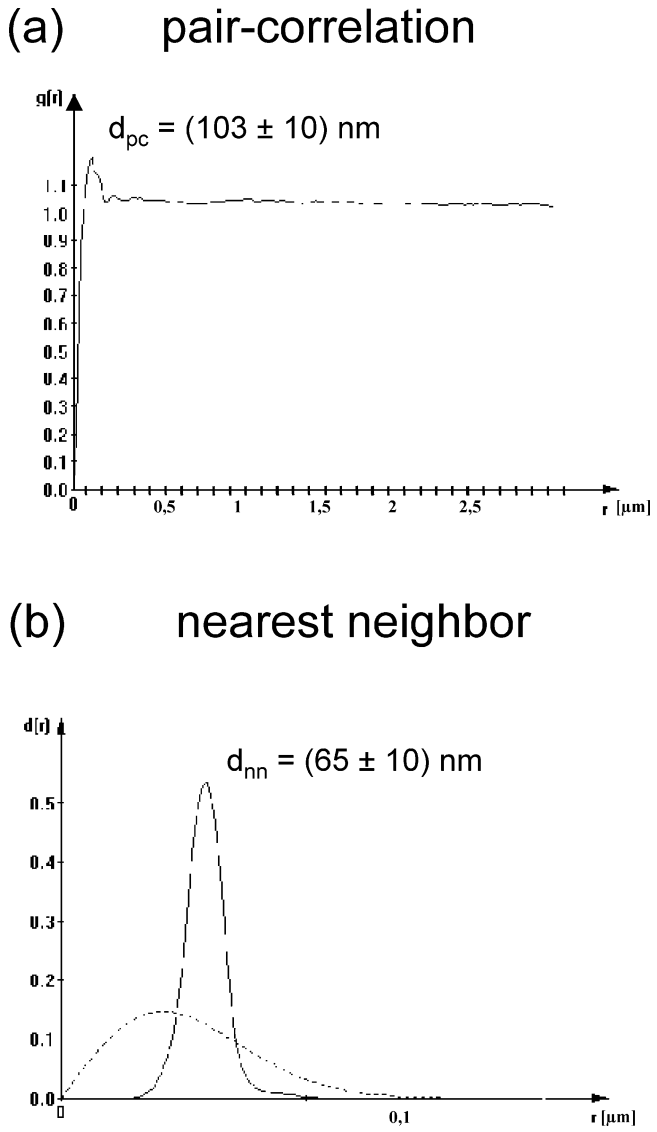

Figure 7. Correlation within the adsorption pattern is shown with the pair-correlation function for Figure 6 (a) and the distribution of the distances of the nearest-neighbor molecules (b). The pair-correlation reveals a main distance of $d_{pc} = 103 \pm 10$ nm. The maximum of the distance distribution of the next neighbors is found at $d_{nn} = 65 \pm 10$ nm. The dashed line in both graphs represent the expectation value for a Poisson field, which is a completely randomly arranged point field.

pattern. The molecules with a given excess charge adhere to the surface and break in the symmetry. The molecules obtain a dipole moment perpendicular to the surface. These dipolar interactions are always present. Figure 8 shows PEI molecules adsorbed from pH = 10 and the corresponding next-neighbor distribution (t_{inc} short). The AFM micrograph reveals single molecules scattered on the surface. However, there is a tendency for agglomeration at high pH values. This behavior fits the expectations that uncharged molecules agglomerate easier due to attractive van der Waals interactions. The intermolecular distances are the same as for lower pH values. The maxima for the distributions of the next neighbor at pH ~ 6 and at pH = 10 overlap within the error. The degree of protonation of the molecules in solution seems to have no influence on the interaction at the surface. This behavior is most likely reflecting the ability of weak polyelectrolytes to adjust their degree of protonation due to the surface properties.[41] At the

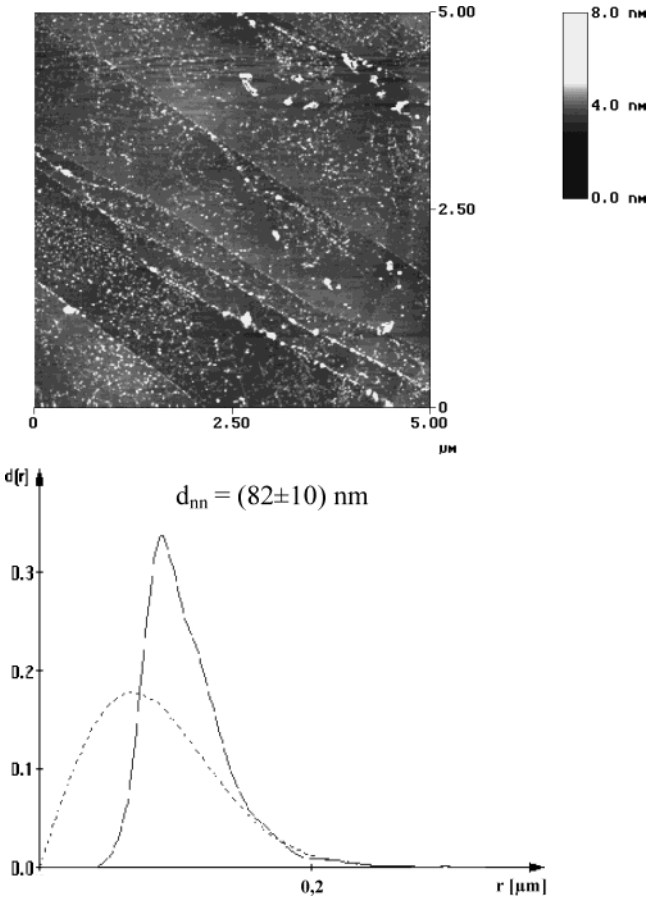

Figure 8. Topography image of PEI molecules adsorbed on graphite from a solution of pH = 10 (top) and the corresponding distribution of the distances of the nearest neighbor (bottom). The value determined is $d_{nn} = 82 \pm 10$ nm. The agglomerates are not considered for the calculations.

surface the molecules feature apparently similar electrostatic properties.

For all samples prepared from pH < 8 and an incubation time of $t_{inc} = 24$ h, similar surface patterns are found. For pH values > 8 the situation changes dramatically. Instead of the single well-separated molecules, as found for the other pH values, the PEI molecules order into domains of parallel polymer strings (Figure 9). The average distance between the strings is found to be $d_{max} = 105$ nm. This value equals the intermolecular distance most frequently determined for pH < 8. Statistical analysis delivers an average height of the structures $\bar{h} = 3 \pm 0.6$ nm, and using section analysis, the average width of the PEI strings is determined to be $\bar{d} = 30 \pm 5$ nm. These values differ from those obtained for single molecules. However, the considerable fluctuations of the measured height of the PEI molecules on graphite do not support the conclusion of two molecules on top of each other.

Another interesting feature is the orientation of the PEI strings. Looking at Figure 9, one can see domains of different orientations. Within these zones the strings are still parallel to each other. A two-dimensional Fourier transformation allows for determination of the symmetry of the adsorption structure. The result of the 2D Fourier transformation of the AFM image in Figure 9 unveils a hexagonal symmetry (Figure 10). Likewise, graphite possesses 6-fold symmetry. It is known that substrates can impose their structure on the adsorbing polyelectrolyte.[48−50] Therefore, it is reasonable to assume that the graphite surface influences or purports the adsorption pattern of the PEI molecules while adsorbing from solution.

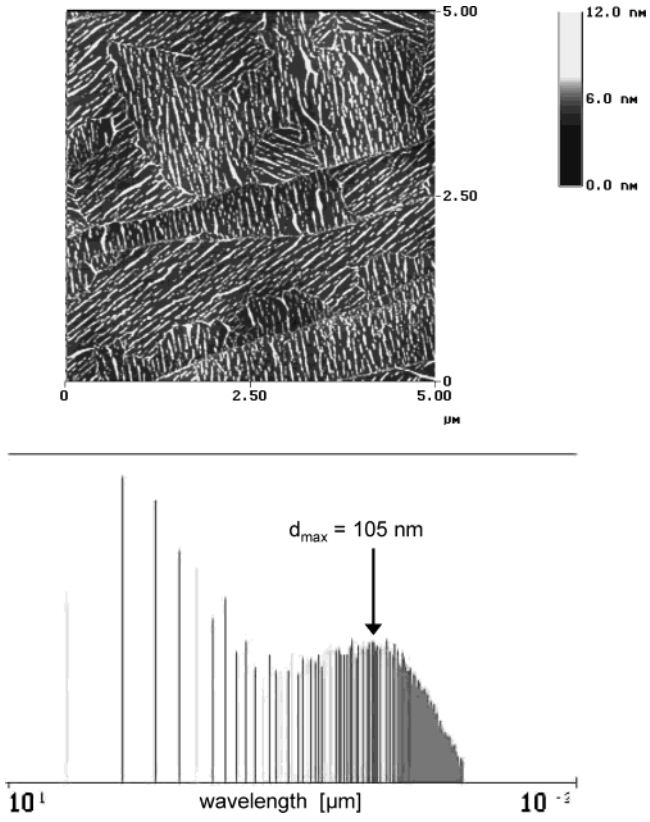

Figure 9. Topography micrograph of the adsorption structure of PEI molecules on graphite. The adsorption was done for $t_{inc} \sim 24$ h from a solution of pH = 11 (top). On the bottom the corresponding spectrum of the existing interstructural distances is displayed as obtained with the DI software. It shows a maximum at a distance of $d_{max} = 105$ nm.

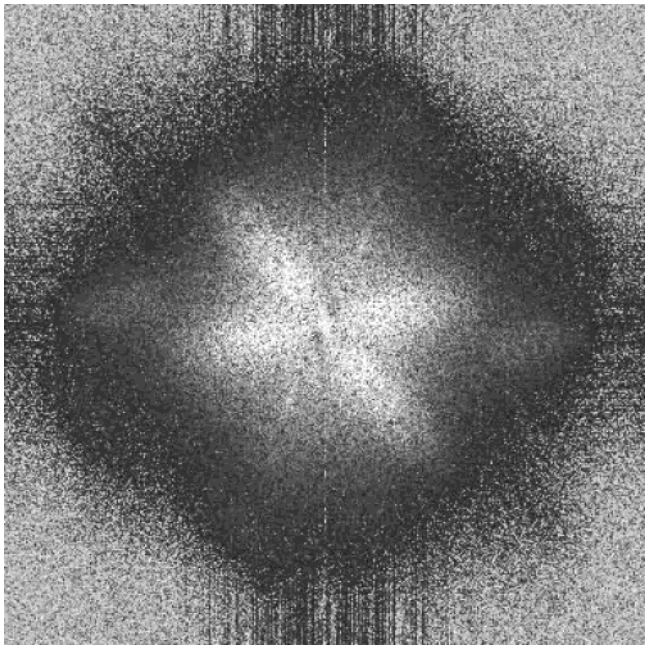

Figure 10. 2D Fourier transformation of the AFM micrograph in Figure 9. The 2D Fourier transformation provides information according to the symmetry of the adsorption structures of the PEI molecules. A 6-fold symmetry is found, which correlates with the hexagonal symmetry of graphite.

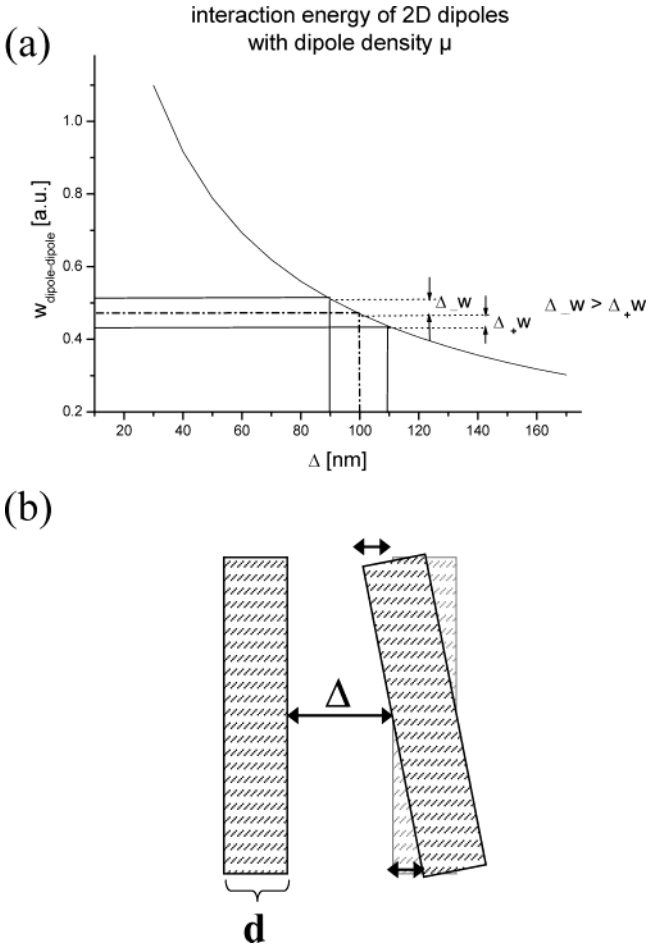

Figure 11. Graph illustrating the interaction energy between two infinite strings of fixed width d in distance Δ (a). Sketch illustrating the tilting of two strings against each other (b). The difference in the energy at the ends of a tilted band is linked to the nonlinear connection between the dipolar energy and the distance between them.

The highly parallel ordering of the PEI strings over hundreds of nanometers can be understood assuming dipolar interactions between the strings, as already mentioned for the short time adsorption patterns. If a dipole density μ, pointing in the same direction as the surface normal, is assigned to each string, the dipolar interaction per length for two infinite long strings with fixed width d at a distance Δ can be expressed as (details in the Appendix)

$$w_{\text{dipole-dipole}} = -\frac{\mu^2}{2\pi\epsilon\epsilon_0}\ln\left(1 - \frac{d^2}{(d+\Delta)^2}\right) \qquad (5)$$

The interaction is repulsive for dipole moments parallel to each other. Figure 11a shows the interaction energy in dependence of the distance between the strings. The logarithmic behavior is the reason for the parallel alignment. This can be seen from the simple case of tilting one string in the direction of another string (Figure 11b). The loss of energy ($\Delta_- w$), while approaching the ends of the strings, overcomes the gain of energy ($\Delta_+ w$) at the other end of the PEI string:

$$\Delta_- w > \Delta_+ w \qquad (6)$$

The driving force for the alignment of the PEI molecules in strings can be attributed to a reduction of the interaction energy within a string. If repulsive interactions are present (due to parallel dipole moments), it is much more efficient to grow as a string then forming a spherical object. The distance between every new molecule and a reference molecule (at the end of the string) is increased, and therefore the interaction is decreased.

An estimation of the interaction energy, or more specifically for the dipolar moment, is achieved by assuming dipole densities and combining them with the experimentally accessible data. Therefore, we presume dipole moments, μ_d, between 0.1 and 3 D. The area attributed per dipole, A_d, was obtained from the calculation of a "Bjerrum length" for dipoles (instead of charges)

$$A_d = \pi\left(\frac{{\mu_d}^2}{4\pi\epsilon\epsilon_0 k_B T}\right)^{2/3} \qquad (7)$$

These areas depend on the dipolar strength of each individual dipole and give each dipole an interaction area, which is assumed to be free of other dipoles. Hence, the minimal distance of the next dipole is at least twice the radius of the dipolar area A_d. This assumption gives a reasonable estimate of the dipoles on a molecular scale. The huge amount of possible dipoles per molecule is decreased by the surface that hinders the molecular groups to move freely. All other moments may cancel. Hence, only the contributions at the interface have to be taken into account. In the case of densely packed dipoles one would expect a more or less hexagonal arrangement of the dipoles perpendicular to the surface of the substrate (Figure 12a). With this presupposition we are able to calculate dipolar interaction energies on the basis of the experimental data (width and length of the strings and the interstring distance). In Figure 12b the energy in units of $k_B T$ is displayed in dependence of the dipole density for three strings of different length. In this case, the dipole density is directly coupled to the dipole moment. The energies obtained exceed the thermal energy. To obtain an estimation of the minimal dipole density, a decoupling of the dipole moment and the area per dipole has to be performed. For a given dipole moment and a fixed string length the density can be calculated at which the dipolar interaction energy equals $k_B T$ (Table 1). With this minimum area for each dipole moment the distance between two dipoles is found to be between 0.14 and 1.1 nm (for the values taken for the dipole moment and the string length). The dipole moments that can be expected for the molecular groups of PEI are $\mu_{H-C} = 0.3$ D for H−C_{al}, $\mu_{H-N} = 1.3$ D for N−H, and $\mu_{NH_3} = 1.47$ D.[51] Our calculations therefore cover a reasonable range of dipolar moments.

The dipolar interaction energy between two PEI bands is big enough to be the driving force in the process of patterning, even though the dipole moments equal those of dipole moments for single molecular groups.

Conclusion

Adsorption of the weak polyelectrolyte PEI onto graphite surfaces is found for diluted solutions of all pH values. An attractive specific interaction between the molecules and the substrate can be concluded from this fact. The influence of electrostatic interactions between single molecules, as well as the intramolecular interactions due to charges, can be observed on the level of single molecules. The adsorption pattern formed by the PEI molecules can be explained with dipolar interac-

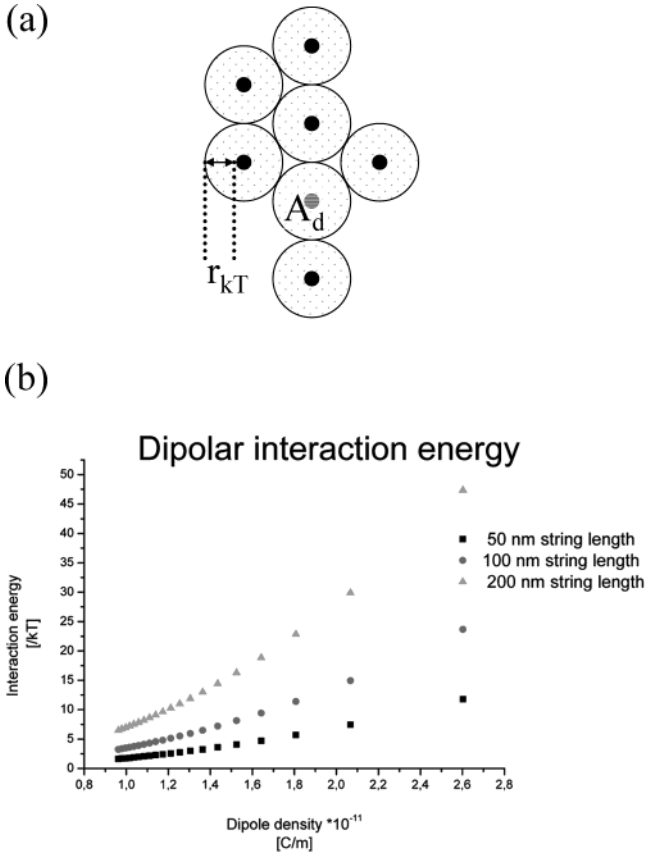

Figure 12. (a) Sketch of the arrangement of the dipoles to each other on the surface. (b) Interaction energy in units of k_BT in dependence of the dipole density μ for three different string lengths. The dipole density is calculated by assuming a dipole moment, and the area per dipole is obtained from a "Bjerrum length" for dipoles.

Table 1. Area per Dipole (in nm²): Calculated A_d per Dipole for Four Given Dipole Moments (in D) and Three Different String Length[a]

	dipole moment [D]			
string length [nm]	0.1	0.5	1	2
100	0.06	0.34	0.62	1.25
500	0.14	0.7	1.39	2.78
1000	0.20	0.98	1.97	3.94

[a] The interaction energy between the strings equals the thermal energy k_BT. This area is a lower barrier for possible dipolar densities.

tions. These interactions can also explain the formation of parallel polymer strings. The orientation of the strings results from the substrate that superimposes its own symmetry to the adsorbing molecules.

We should also mention that the dipole densities assumed here are not extraordinarily large. Thus, one also expects similar adsorption behavior for other macromolecules or particles, like proteins or quantum dots.

Acknowledgment. We thank the BMBF (Project Number 03C0291C/5) for financial support. We are indebted to A. Heilig for the AFM measurements and to Dr. C. Faul for help with language. Rene Hoogendam (Department of Physical and Colloid Chemistry, Wageningen Agricultural University, Netherlands) is warmly acknowledged for providing information for the calculation of the adsorbed amounts.

Appendix

Calculation of the Interaction Energy between Two Areas of Dipole Density μ. To obtain the interaction energy between two infinite long strings of fixed width and dipole density μ, which is oriented perpendicular to the surface, eq A.1 has to be solved:

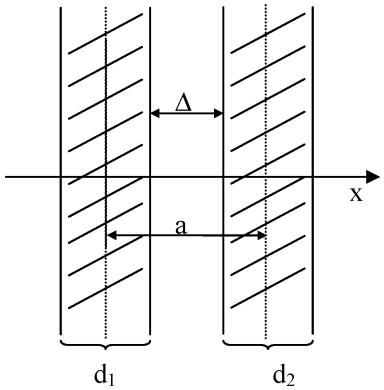

Figure 13. Sketch of two infinite long strings (y-direction). They feature a fixed width d and are located at a distance Δ. The distance between the center lines of the strings is represented by a. For application to the PEI/graphite system, the width of the strings can be assumed equal ($d_1 = d_2$). In addition, the polydispersity is not taken into account. The width is set homogeneous.

$$w_{\text{dipole-dipole}} = \frac{\mu^2}{4\pi\epsilon\epsilon_0}\int dA_1 \int dA_2 \frac{1}{r_{12}^3} \qquad \text{(A.1)}$$

A_i is the area of each string, ϵ and ϵ_0 are the medium's dielectric constant and the permittivity of free space, respectively, and r_{12} is an arbitrary distance between the strings.

First, consider the interaction between two infinite long lines per unit length. The interaction energy $\bar{w}$ is expressed with

$$\bar{w} = \int_{-\infty}^{\infty} \frac{1}{\sqrt{((x-x_0)^2+y^2)^3}}\,dy = \frac{y}{(x-x_0)^2\sqrt{(x-x_0)^2+y^2}}\Bigg|_{-\infty}^{\infty} = \frac{2}{(x-x_0)^2} \qquad \text{(A.2)}$$

This result is extended to infinite long strings of fixed width d_i by a second integration in the x-direction. The strings are located at a distance a of the center lines (Figure 13).

$$w_{\text{dipole-dipole}} = \frac{2\mu^2}{4\pi\epsilon\epsilon_0}\int_{-d_2/2}^{d_2/2} dx_2 \int_{-d_1/2}^{d_1/2} dx_1 \frac{1}{(a+x_1+x_2)^2}$$

$$= -\frac{\mu^2}{\pi\epsilon\epsilon_0}\int_{-d_2/2}^{d_2/2} dx_2 \left[\frac{1}{2a+d_1+2x_2} - \frac{1}{2a-d_1+2x_2}\right]$$

$$= \frac{\mu^2}{2\pi\epsilon\epsilon_0}[[\ln(2a-d_1+d_2) - \ln(2a-d_1-d_2)] - \ln(2a+d_1+d_2) - \ln(2a+d_1-d_2)] \qquad \text{(A.3)}$$

$$w_{\text{dipole-dipole}} = \frac{\mu^2}{2\pi\epsilon\epsilon_0}\left[\ln\left(1-\frac{d_1-d_2}{2a}\right)-\ln\left(1-\frac{d_1+d_2}{2a}\right)-\ln\left(1+\frac{d_1+d_2}{2a}\right)+\ln\left(1+\frac{d_1-d_2}{2a}\right)\right] \quad \text{(A.4)}$$

With $d_1 = d_2 = d$ two terms in (A.4) are zero, and we obtain

$$w_{\text{dipole-dipole}} = \frac{\mu^2}{2\pi\epsilon\epsilon_0}\left[-\ln\left(1+\frac{d}{a}\right)-\ln\left(1-\frac{d}{a}\right)\right] \quad \text{(A.5)}$$

which is with $a = d + \Delta$ transformed in

$$w_{\text{dipole-dipole}} = \frac{\mu^2}{2\pi\epsilon\epsilon_0}\left[-\ln\left(1+\frac{d}{d+\Delta}\right)-\ln\left(1-\frac{d}{d+\Delta}\right)\right] \quad \text{(A.6)}$$

Extension of the logarithmic arguments (A.6) can be further simplified. In the end, an expression for the interaction energy is obtained for two strings of width d at a distance Δ:

$$w_{\text{dipole-dipole}} = -\frac{\mu^2}{2\pi\epsilon\epsilon_0}\ln\left(1-\frac{d^2}{(d+\Delta)^2}\right) \quad \text{(A.7)}$$

Note Added after ASAP

This article was published ASAP on 10/21/03 with mistakes in calculations in the Appendix. These were corrected, and subsequent corrections needed to be made in eq 5, Figure 12, and data in the second to last paragraph before the Conclusion. The paper was reposted to the Web on 11/18/03.

References and Notes

(1) Horn, D.; Linhart, F. Retention Aids. In *Paper Chemistry*, 2nd ed.; Roberts, J., Ed.; Blackie Academic & Professional: Glasgow, 1996; p 64.
(2) Alince, B.; Vanerek, A.; vandeVen, T. G. M. *Ber. Bunsen-Ges.* **1996**, *100*, 954.
(3) Evers, O. A.; Fleer, G. J.; Scheutjens, J.; Lyklema, J. *J. Colloid Interface Sci.* **1986**, *111*, 446.
(4) Therkelsen, G. H. Carrageenan. In *Industrial Gums-Polysaccharides and Their Derivatives*, 3rd ed.; Whistler, R. L., BeMiller, J. N., Eds.; Academic Press: New York, 1993; p 145.
(5) D'Souza, S. F.; Kamath, N. *Appl. Microbiol. Biotechnol.* **1988**, *29*, 136.
(6) Nichol, C. A.; Yang, D.; Humphrey, W.; Ilgan, S.; Tansey, W.; Higuchi, T.; Zareneyrizi, F.; Wallace, S.; Podoloff, D. A. *Drug Delivery* **1999**, *6*, 187.
(7) Godbey, W. T.; Wu, K. K.; Mikos, A. G. *J. Controlled Release* **1999**, *60*, 149.
(8) Hellweg, T.; Henry-Toulme, N.; Chambon, M.; Roux, D. *Colloids Surf., A* **2000**, *163*, 71.
(9) Bohmer, M. R.; Evers, O. A.; Scheutjens, J. *Macromolecules* **1990**, *23*, 2288.
(10) Claesson, P. M.; Paulson, O. E. H.; Blomberg, E.; Burns, N. L. *Colloids Surf., A* **1997**, *123*, 341.
(11) Lowack, K.; Helm, C. A. *Macromolecules* **1998**, *31*, 823.
(12) Pfau, A.; Schrepp, W.; Horn, D. *Langmuir* **1999**, *15*, 3219.
(13) Blaakmeer, J.; Bohmer, M. R.; Cohen-Stuart, M. A.; Fleer, G. J. *Macromolecules* **1990**, *23*, 2301.
(14) Silberberg, A. *J. Chem. Phys.* **1968**, *48*, 2835.
(15) Roe, R. J. *Bull. Am. Phys. Soc.* **1974**, *19*, 288.
(16) Geffroy, C.; Labeau, M. P.; Wong, K.; Cabane, B.; Stuart, M. A. C. *Colloids Surf., A* **2000**, *172*, 47.
(17) Kawaguchi, M.; Saito, W.; Kato, T. *Macromolecules* **1994**, *27*, 5882.
(18) Caruso, F.; Lichtenfeld, H.; Donath, E.; Mohwald, H. *Macromolecules* **1999**, *32*, 2317.
(19) Ladam, G.; Schaad, P.; Voegel, J. C.; Schaaf, P.; Decher, G.; Cuisinier, F. *Langmuir* **2000**, *16*, 1249.
(20) Serizawa, T.; Takeshita, H.; Akashi, M. *Langmuir* **1998**, *14*, 4088.
(21) Harris, J. J.; Bruening, M. L. *Langmuir* **2000**, *16*, 2006.
(22) Serizawa, T.; Taniguchi, K.; Akashi, M. *Colloids Surf., A* **2000**, *169*, 95.
(23) Reihs, K. *Thin Solid Films* **1995**, *264*, 135.
(24) Borkovec, M.; Koper, G. J. *Macromolecules* **1997**, *30*, 2151.
(25) Poptoshev, E.; Claesson, P. M. *Langmuir* **2002**, *18*, 2590.
(26) Dick, C. R.; Ham, G. E. *J. Macromol. Sci., Chem.* **1970**, *A4*, 1301.
(27) Schuch, H. BASF AG, Ludwigshafen, Germany, personal communication.
(28) Park, I. H.; Choi, E.-J. *Polymer* **1996**, *37*, 313.
(29) Dalluge, R.; Haberland, A.; Zaitsev, S.; Schneider, M.; Zastrow, H.; Sukhorukov, G.; Bottger, M. *Biochim. Biophys. Acta* **2002**, *1576*, 45.
(30) Treweek, G. P.; Morgan, J. J. *J. Colloid Interface Sci.* **1977**, *60*, 258.
(31) Horn, D. Polyethylenimine-Physicochemical Properties and Applications. In *Polymeric Amines and Ammonium Salts*; Goethals, E. J., Ed.; Pergamon Press: Oxford, 1980; p 333.
(32) Winnik, M. A.; Bystryak, S. M.; Chassenieux, C.; Strashko, V.; Macdonald, P. M.; Siddiqui, J. *Langmuir* **2000**, *16*, 4495.
(33) Andersson, M. M.; Hatti-Kaul, R.; Brown, W. *J. Phys. Chem. B* **2000**, *104*, 3660.
(34) Dahlgren, M. A. G.; Waltermo, A.; Blomberg, E.; Claesson, P. M.; Sjostrom, L.; Akesson, T.; Jonsson, B. *J. Phys. Chem.* **1993**, *97*, 11769.
(35) Bremmell, K. E.; Jameson, G. J.; Biggs, S. *Colloids Surf., A* **1998**, *139*, 199.
(36) Schneider, M.; Zhu, M.; Papastavrou, G.; Akari, S.; Mohwald, H. *Langmuir* **2002**, *18*, 602.
(37) Meszaros, R.; Thompson, L.; Bos, M.; de Groot, P. *Langmuir* **2002**, *18*, 6164.
(38) Drifford, M.; Dalbiez, J.-P. *Biopolymers* **1985**, *24*, 1501.
(39) Motschmann, H.; Stamm, M.; Toprakcioglu, C. *Macromolecules* **1991**, *24*, 3681.
(40) Schmitt, J.; Machtle, P.; Eck, D.; Mohwald, H.; Helm, C. A. *Langmuir* **1999**, *15*, 3256.
(41) Fleer, G. J.; Cohen Stuart, M. A.; Scheutjens, J.; Cosgrove, T.; Vincent, B. *Polymers at Interfaces*, 1st ed.; Champman & Hall: London, 1993.
(42) Stuart, M. A. C.; Hoogendam, C. W.; deKeizer, A. *J. Phys.: Condens. Matter* **1997**, *9*, 7767.
(43) Cohen Stuart, M. A.; Fleer, G. J.; Lyklema, J.; Norde, W.; Scheutjens, J. *Adv. Colloid Interface Sci.* **1991**, *34*, 477.
(44) Linse, P. *Macromolecules* **1996**, *29*, 326.
(45) Fleer, G. J. *Ber. Bunsen-Ges.* **1996**, *100*, 936.
(46) Stoyan, D. Gewichtung der statistischen Korrelationen.
(47) Stoyan, D.; Stoyan, H. *Fraktale-Formen-Punktfelder: Methoden der Geometrie-Statistik*, 1st ed.; Akademie Verlag GmbH: Berlin, 1992.
(48) Cyr, D. M.; Venkataraman, B.; Flynn, G. W. *Chem. Mater.* **1996**, *8*, 1600.
(49) Liu, J. F.; Ducker, W. A. *Langmuir* **2000**, *16*, 3467.
(50) Loi, S.; Butt, H. J.; Hampel, C.; Bauer, R.; Wiesler, U. M.; Mullen, K. *Langmuir* **2002**, *18*, 2398.
(51) Falbe, J.; Regitz, M. *Römpp Chemie Lexikon*, 9th ed.; Georg Thieme Verlag: Stuttgart, 1995.
(52) Zhu, M.; Schneider, M.; Papastavrou, G.; Akari, S.; Möhwald, H. *Langmuir* **2001**, *17*, 6471.
(53) Bloys van Treslong, C. J.; Staverman, A. J. *J. R. Neth. Chem. Soc.* **1974**, *93*, 171.

MA0345293